Published in final edited form as:

Mucosal Immunol. 2014 March ; 7(2): 304–314. doi:10.1038/mi.2013.48.

Imaging murine NALT following intranasal immunization with flagellin-modified circumsporozoite protein malaria vaccines

Adéla Nacer, Ph.D.[1,$], **Daniel Carapau, Ph.D.**[1,#], **Robert Mitchell**[1], **Abby Meltzer**[1], **Alan Shaw, Ph.D.**[2], **Ute Frevert, DVM, Ph.D.**[1], and **Elizabeth H Nardin, Ph.D.**[1,*]

[1]Division of Medical Parasitology, Department of Microbiology, New York University School of Medicine, New York, NY 10010, USA

[2]VaxInnate Corporation, Cranbury, NJ 08512, USA

Abstract

Intranasal (IN) immunization with a *Plasmodium* circumsporozoite (CS) protein conjugated to flagellin, a TLR5 agonist, was found to elicit antibody mediated protective immunity in our previous murine studies. To better understand IN elicited immune responses, we examined the nasopharynx-associated lymphoid tissue (NALT) in immunized mice and the interaction of flagellin-modified CS with murine dendritic cells (DC) *in vitro*. NALT of immunized mice contained a predominance of germinal center (GC) B cells and increased numbers of CD11c+ DC localized beneath the epithelium and within the GC T cell area. We detected microfold (M) cells distributed throughout the NALT epithelial cell layer and DC dendrites extending into the nasal cavity which could potentially function in luminal CS antigen uptake. Flagellin-modified CS taken up by DC *in vitro* was initially localized within intracellular vesicles followed by a cytosolic distribution. Vaccine modifications to enhance delivery to the NALT and specifically target NALT APC populations will advance development of an efficacious needle-free vaccine for the 40% of the world's population at risk of malaria.

Keywords

P. falciparum; flagellin; Intranasal; vaccine

Introduction

Malaria, a vector borne disease caused by parasites of the genus *Plasmodium*, remains a major global health problem (http://www.who.int/malaria/world_malaria_report_2011/en/).

[*]Corresponding author: Elizabeth Nardin, Ph.D. Division of Medical Parasitology, Department of Microbiology, New York University School of Medicine, 341 E 25 St, New York, NY 10010, Tel: 212-263-6819, Fax: 212-263-8116: elizabeth.nardin@nyumc.org.

[$]**Current addresses**: Adéla Nacer: Biologie des Interactions Hôte-Parasite, Institut Pasteur, 25 rue du Docteur Roux, 75015 Paris, France: adela.nacer@pasteur.fr

[#]Daniel Carapau: Unidade de Malária, Instituto de Medicina Molecular, Universidade de Lisboa, Lisboa, Portugal: dcarapau@fm.ul.pt

Alan Shaw, PhD, Vedantra Pharmaceuticals, Inc., 1 Broadway, Cambridge, MA 02142: Arshaw1@mac.com

Disclosure: AN, DC, RM, AM, UF and EN declare no conflict of interest. A. Shaw was employed by VaxInnate at the time of these studies.

Despite important progress made by vector control initiatives and new artemisinin-based chemotherapy, the morbidity and mortality associated with this disease remain high, with an estimated 216 – 500 million episodes of malaria and 655,000 deaths each year. The need for a vaccine remains urgent, especially considering the recent reports of parasite artemisinin drug resistance and vector pyrethroid resistance.

The complex life cycle of *Plasmodium* will require a multifaceted approach to control/eradicate malaria. Optimism for development of vaccines as part of this multipronged approach has been raised by a recent phase III clinical trial of a vaccine based on a major sporozoite surface antigen, the circumsporozoite (CS) protein [1, 2]. This CS-based vaccine, termed RTS,S, targets the parasite at its pre-erythrocytic stages with the goal of preventing development of the erythrocytic stages responsible for clinical disease. The pre-erythrocytic stages are attractive immune targets as sporozoites inoculated by the mosquito vector and the exoerythrocytic forms that subsequently develop in the liver can be inhibited by antibody and by cellular immune responses, respectively. Successful prevention of the intra-erythrocytic cycle also will prevent development of parasite sexual stages responsible for transmission to the mosquito vector.

A key requirement for induction of potent humoral and cellular immunity is the dendritic cell (DC), which bridges the innate and adaptive immune response. Toll-like receptor (TLR) agonists that can be linked to antigens, such as the TLR 5 agonist flagellin, function as strong adjuvants that induce maturation of DC and upregulation of costimulatory molecules required for initiation of adaptive immunity . Viral and bacterial antigens linked to flagellin have shown promise as parenteral and mucosal vaccines in murine studies and clinical trials [3-8].

In a recent murine study, we demonstrated the immunogenicity, as well as the *in vitro* and *in vivo* protective efficacy of antibodies elicited by a recombinant *P. falciparum* circumsporozoite (CS) protein modified with the TLR5 ligand flagellin when delivered either subcutaneously (SC) or intranasally (IN) (Carapau, Mitchell, Nacer, Shaw, Othoro, Frevert et al, unpublished). The vaccine was comprised of an *E. coli* expressed recombinant *Salmonella enterica* Typhimurium flagellin B protein, either full length (STF2) or truncated to remove the hinge region (STF2Δ), fused with T and B cell epitopes of *P. falciparum* CS protein or a nearly full length CS protein (Figure 1). Sera of mice immunized IN or SC with the flagellin-modified CS constructs had similar levels of predominantly IgG1 antibodies to CS or to flagellin. Antibody responses were dependent on flagellin as minimal or no antibodies to either CS or flagellin were obtained in *tlr5* −/− mice. Immune sera from the IN immunized mice neutralized sporozoite infectivity *in vitro* when pre-incubated with viable transgenic *PfPb* sporozoites expressing *P. falciparum* CS repeats [9]. Consistent with the *in vitro* findings, IN immunized mice challenged by exposure to the bites of *PfPb*-infected mosquitoes had a >90% decrease in parasite 18S rRNA in liver extracts obtained 40h post-challenge. In contrast, mice immunized SC with flagellin-modified CS had lower levels of sporozoite-neutralizing antibodies detectable both *in vitro* and *in vivo*. These data provide the first demonstration of protective antibody mediated immunity against sporozoites elicited by IN immunization with a flagellin-modified-*P. falciparum* CS and support the

potential of developing a scalable, low cost, needle-free malaria vaccine for the 40% of the world's population currently at risk of malaria.

In an effort to better understand the cellular environment in which protective immunity develops following IN immunization with flagellin-modified CS proteins, we analyzed the cell composition and structure of the nasopharynx-associated lymphoid tissue (NALT). Previous studies have demonstrated the immunogenicity of multiple malaria antigens when administered IN [10-13], but the interaction of malaria antigen with NALT has not been examined. The murine NALT resembles other non-encapsulated lymphoid organs, such as the Peyer's Patches (PP) of the gut-associated lymphoid tissue (GALT). However, murine NALT differs from GALT in terms of organogenesis as it begins to develop only after birth and does not require lymphotoxin-α or the retinoic acid receptor related orphan receptor-γ transcription factor (ROR-γ t) as is required for GALT [14]. In contrast to lymph nodes, NALT and other mucosa-associated lymphatic tissues such as GALT and the bronchus-associated lymphoid tissue (BALT), do not contain afferent lymphatics; instead, antigen transport into the lymphoid compartment requires specialized cells that transcytose or directly sample luminal antigen content.

In the current studies, we have used flow cytometry and confocal microscopy to examine NALT of mice immunized IN with flagellin-modified CS constructs. We demonstrate a cellular milieu characterized by expansion of B and T lymphocytes and influx of CD11+ DC into the NALT *in vivo*, and a pattern of CS antigen uptake into murine DC *in vitro*, that potentially play key roles in vaccine-induced immune responses.

Results

NALT structure and composition

Mice were immunized IN with flagellin-modified CS constructs previous shown to be immunogenic when delivered SC or IN to Balb/c or C57BL/6 mice (Carapau, Mitchell, Nacer, Shaw, Othoro, Frevert et al, unpublished) (Figure 1). STF2Δ.CS was comprised of nearly full-length *P. falciparum* CS protein fused to a truncated flagellin, which lacks 300 aa of the hypervariable hinge region (STF2Δ), while STF2.(T1BT*)$_{4\times}$ contained four copies of immunodominant T and B cell epitopes from the *P. falciparum* CS protein, designated T1BT*, fused to full-length flagellin (STF2). The murine NALT are a pair of lymphoid aggregates located on the soft palate on either side of the nasal passages, optimally sited to detect inhaled foreign material (Figure 2). The size of the NALT in mice immunized IN with either of the flagellin-modified CS constructs was increased when compared to naïve mice when examined macroscopically (Figure 3). Measurements of the NALT area from trichrome stained sections showed an approximately 2-fold increase in the NALT of immunized as compared to naïve mice. Enlargement of the NALT was due to the presence of the flagellin TLR5 agonist, as IN immunization with flagellin alone elicited a similar increase in size of the NALT (data not shown).

NALT-associated lymphoid cell populations

Flow cytometric analysis of the NALT cell populations in naïve C57BL/6 mice revealed that the predominant NALT cells were B cells, while CD3+ T cells and CD11c+ DC accounted for 10% and 3%, respectively (Figure 4). While IN immunization with the flagellin-modified CS constructs elicited an ∼2-fold increase in NALT size associated with increased cell numbers (Figure 3), the ratio of T:B cells in the IN immunized mice was similar to the naïve mice with a marked predominance of B cells (Figure 4 A, B). A low T:B ratio was also found in NALT from BALB/c mice immunized IN with flagellin-modified CS (data not shown), consistent with the previous observed comparable anti-repeat antibody titers following IN immunization with flagellin-modified CS in both BALB/c and C57BL/6 mice (Carapau, Mitchell, Nacer, Shaw, Othoro, Frevert et al, unpublished).

In contrast, while the ratio of T and B cells remained similar in naïve and immunized mice, there was a dose dependent increase in percentage of CD11c+ DC in the NALT of the immunized C57BL/6 mice (Figure 4C). A modest increase (∼50%) in CD11+ DC was observed following the 1^{st} immunization with STF2Δ.CS (3.1%) or STF2Δ (2.8%) as compared to naïve (2.0%). Following the 4^{th} immunization, there was a 2-3 fold increase in percentage of CD11+ DC observed in STF2Δ.CS (7.1%) or STF2Δ (6.0%) immunized mice as compared to naïve mice (2.2%) [$P < 0.05$]. The >2-fold increase in CD11c+ DC in the mice immunized with flagellin (STF2Δ) only indicated that the increase in DC was due to flagellin stimulation of NALT.

Consistent with the flow cytometric analysis of NALT cell populations, immunolabeling of freshly excised snap-frozen and fixed NALT cryosections confirmed that the majority of lymphocytes in the naïve NALT were B220+ B cells (Figure 5). Because the position of B and T cell regions within the NALT parenchyma is variable [15], NALTs were analyzed longitudinally. Mice immunized with STF2.$(T1BT^*)_{4\times}$, developed increased numbers of CD3+ T cells that were clearly detected in the enlarged NALT of immunized mice.

Increased numbers of CD11c+ DC were also evident in the immunolabeled sections of NALT from STF2.$(T1BT^*)_{4\times}$ immunized mice (Figure 6). Immunolabeled whole NALT from STF2Δ.CS or flagellin only (STF2Δ) immunized mice also showed similar increases in DC (Figure S1). The majority of the DC was detected just below the NALT columnar epithelium and in the T cell zone at the periphery of B cell follicles where DC interaction with T cells would be initiated. When analyzed by flow cytometry, 63.06% of the DC from the mice immunized with STF2.$(T1BT^*)_{4\times}$ were CD86+, compared to 26.5% of STF2 immunized mice and 21.3% of naïve mice (data not shown). While flagellin with or without CS enhanced CD86 expression on human or murine DC *in vitro* (Carapau, Mitchell, Nacer, Shaw, Othoro, Frevert et al, unpublished), the higher levels of CD86 expression on NALT DC from STF2. $(T1BT^*)_{4\times}$ immunized mice suggest that the presence of CS in the chimeric flagellin may enhance DC activation within the NALT *in vivo*. Alternatively, the murine cell line used for our *in vitro* studies may not adequately reflect DC phenotypes elicited by flagellin/TLR5 interactions in the epithelial and lymphoid tissues of the NALT.

NALT microvasculature

To visualize routes by which DC would migrate to and enter the NALT, sections were labeled with anti-PECAM-1 to detect endothelia of blood vessels and with anti-LYVE-1, a marker for lymphatic endothelia [16]. While blood microvessels were distributed throughout the lymphatic tissue of the NALT, lymphatic vessels were primarily located in the posterior portion of the NALT and oriented longitudinally along the connective tissue of the soft palate underlying the NALT (Figure 7). Consistent with the lack of afferent lymphatics in NALT, this vascular distribution suggests haematogenous influx of DC via high endothelial venules. Following antigen uptake, DC could directly interact with T cells within the NALT, or exit via efferent lymphatics towards the draining cervical lymph node (LN), to induce adaptive immune responses. Consistent with a role of the dLN in the immune responses, we found the cervical, superficial parotid and mandibular LN were increased in size following immunization with flagellin or flagellin modified CS (data not shown).

NALT epithelium, DC, and M cells

When the epithelial layer was examined, H&E-stained paraffin sections demonstrated the ciliated columnar epithelia lining the nasal cavity and the follicular associated epithelial cells (FAE) covering the lymphoid dome containing B and T lymphocytes (Figure 8). The columnar epithelia were interspersed with numerous goblet cells, which were less prominent in the FAE covering the NALT (Figure 8, A versus B). Small non-ciliated cells, microfold (M) cells interspersed between the ciliated columnar NALT epithelium were detected in trichrome-stained paraffin sections (Figure 8, C and D) and in toluidine blue-stained Epon sections (Figure 8E). Labeling with an M cell-specific lectin, *Griffonia simplicifolia* GS-IB_4[17], confirmed the presence of M cells in the epithelial layer overlaying the lymphoid aggregates of the NALT (Figure 8G).

Of interest, cells of a dendritic morphology were found that appeared to extend dendrites across the epithelium into the nasal cavity (Figure 8C, D and F). These cells are considered DC based on their shape, location in close proximity to the epithelium and staining with anti-CD11c antibody (Figure 8H). DC within the gut are known to extend dendrites across the intact epithelium to sample luminal antigens [18, 19]. However, CS antigen could not be detected within DC in freshly excised snap-frozen and fixed NALTs immunolabeled with MAB 2A10, specific for *P. falciparum* CS repeats, at 10 min, 30 min, 1 h, or 3 h post IN immunization. Most likely our staining methods were not sensitive enough to detect the limited amount of antigen these cells internalize *in vivo*.

DC uptake of flagellin-modified CS *in vitro*

Since we were unable to detect intracellular CS protein in tissue sections, we examined the uptake of flagellin-modified CS by DC *in vitro* using murine bone marrow derived dendritic cells (BMDC). To synchronize antigen uptake, BMDC were incubated with or without 100 μg/ml of flagellin-modified CS for 30 min on ice followed by 30 min incubation at 37°C. Both STF2.$(T1BT^*)_{4\times}$ and STFΔ.CS were taken up by DC within 30 min, as measured by labeling with mAb 2A10 specific for *P. falciparum* CS (Figure 9A). A stronger intracellular signal was observed in BMDC incubated with STFΔ.CS compared to STF2.$(T1BT^*)_{4\times}$. However these higher levels may reflect increased binding of mAb 2A10 due to the more

numerous repeats present in full length CS protein, which contains 44 tetramer repeats, as compared to 24 tetramer repeats present in the STF2.$(T1BT^*)_{4\times}$ construct (Figure 1).

The intracellular distribution of malaria antigen within the DC ranged from small vesicles, presumably early endosomes, to larger vesicles (possibly late endosomes), as well as distribution throughout the cytosol (Figure 9B). After 30 min of incubation with STFΔ.CS, the majority (55%) of the CS+ DC had a cytosolic labeling pattern, suggesting that flagellin-modified CS readily translocated from the endocytic compartment into the cytosol of DC.

Quantification of the BMDC staining profiles indicated that intracellular distribution of flagellin-modified CS was dose dependent (Figure 9C). When labeled with mAb 2A10+, BMDC incubated with 10 μg of STF $(T1BT^*)_{4\times}$ had 60% CS+ positive cells while cells incubated with 100 μg/ml were 75% antigen positive. Cytosolic CS was detected in 5.13% of BMDC incubated with the high dose of antigen (100 μg/ml), while none of the cells at the lower concentration had detectable CS in the cytosol. The proportion of vesicular and/or cytosolic intracellular staining patterns differed for the two flagellin-CS constructs. BMDC incubated with 100 μg/ml STFΔ.CS had higher levels of positive cells (88%) with higher levels of cytosolic distribution (13%), when compared to DC cultures incubated with STF2.$(T1BT^*)_{4\times}$. While these differences may reflect heterogeneity in activation states or DC subsets within the BMDC cultures, increased detection of STFΔ.CS by MAB 2A10, as noted above, is also a possible explanation for these differences.

The presence of cytosolic flagellin-modified CS led to alterations in BMDC morphology. The cells exhibiting vesicular antigen remained well spread, with a morphology similar to cells that did not take up flagellin-modified CS (Figure S2 B, C). In contrast, cells with a cytosolic antigen appeared rounded. In confocal 3D data isosurfaces representing the intracellular distribution of CS protein, cells with vesicular CS protein are well spread (Figure S2 E) while cells containing large amounts of cytosolic antigen appeared shrunken or rounded and contained small pycnotic nuclei (Figures S2 F, G), consistent with either apoptosis or pyroptosis.

Discussion

Intranasal immunization, in addition to providing a needle-free vaccine, has the advantage of targeting a highly vascularized, easily accessible lymphoid tissue with a large absorption surface. Our previous study had found that IN immunization with flagellin-modified CS constructs elicited systemic antibody responses that provided superior protection compared to SC immunization (Carapau, Mitchell, Nacer, Shaw, Othoro, Frevert et al, unpublished). Responses were dependent on presence of the flagellin adjuvant, as minimal or no antibody to CS or flagellin was obtained in *tlr 5* −/− mice or following IN immunization with T1BT* peptide without flagellin, consistent with the adjuvant dependence of immune responses to CS proteins or peptides delivered by parenteral injection [20, 21].

To better understand the immune mechanisms functioning in intranasal immunization, we examined the NALT structure and cell populations of mice immunized with flagellin-modified CS constructs. When examined at various time points post immunization, using

flow cytometry and confocal microscopy, the cellular composition in the NALT was found to differ from lymph nodes. A predominance of B cells was observed for NALT of mice immunized with flagellin-modified CS (Figures 4 and 5), similar to the predominance of B cells in PP, potentially making NALT a privileged site for antibody production. Although the NALT doubled in size following immunization with flagellin-modified CS constructs, a low T:B cell ratio persisted with a predominant population of B cells. Previous reports showed that clonal expansion of B and T cells in the NALT could occur in a manner that maintains this low T:B ratio [15].

Immunization with flagellin-modified CS lead to an increase in numbers of CD11c+ DC located under the single-layer epithelium of the NALT (Figures 4, 6, 8 **and** S1). The interaction of antigen with TLR5 expressed on NALT FAE [22] may stimulate chemokine secretion to increase influx of DC Expression of occludin and certain claudins has been implicated in DC entry into the epithelium, while ZO-1 upregulation was proposed to allow DC detachment for migration to the draining lymph node (dLN) [18]. DC, in addition to functioning as APC for T and B cells within the NALT, could therefore also transport malaria antigen via efferent lymphatics (Figure 7) to the dLN. In addition to the increase in size of the NALT, we found the cervical, superficial parotid, and mandibular LN increased in size following immunization with flagellin or flagellin-modified CS. Previous studies using OVA-tagged *S. pyogenes* and *L. murinus*, and OT-II cells, show a higher frequency of T cell division in NALT than in cervical LN in early responses, followed by the later expansion in the cervical dLN, suggesting that NALT can serve as the inductive site for CD4+ T cells, as well as B cells [23, 24].

Antigen uptake into the NALT is thought to occur via several routes: 1) transcytosis through M cells, 2) transport across the columnar epithelia, and 3) direct luminal sampling via DC dendrites. Our staining of NALT sections detected GS-IB_4 lectin-positive M cells in the epithelial layer that may function in the uptake of flagellin-modified CS (Figure 8), similar to their role in antigen transport and the development of mucosal immune responses in intestinal PP [25]. The unique M cell pocket, formed by invagination of the epithelial basal membrane, is thought to function as an intraepithelial docking site for lymphocytes, macrophages and DC. In addition to antigen uptake, transcriptional analysis has detected TLR5 expression in M cells, as well as follicular associated epithelium cells of PP [22]. GALT M cells and FAE have been shown to secret C-C ligand chemokines (CCL9, CCL25, and CCL20) that attract dendritic cells. CCL20 in GALT is upregulated in response to danger signals, such as flagellin on *S. enterica* Typhimurium [26]. Interaction of flagellin-modified CS with TLR 5 on NALT M cells or FAE may induce chemokines that attract DC to the NALT epithelium.

In the current studies, in addition to the increased numbers of DC, intercellular dendrites of DC extending beyond the ciliated epithelial cell layer were noted in NALT from mice immunized with flagellin-modified CS (Figure 8 C, D and F). These structures were consistent with previously reported trans-epithelial “balloon” shaped dendrites extended by CD11c+ DC into the gut lumen in C57BL/6 mice [19, 27]. Direct luminal sampling of nasal cavity via DC dendrites is consistent with current models for sampling of bacteria in gut or airways [28, 29]. Dendrite extensions of DC within nasal tissue of patients suffering allergic

rhinitis have also been reported [30]. The number of DC dendrites has been shown to increase in response to presence of Salmonella in the gut that was mediated via fractalkine receptor (CX3CR1)/CX3CL1 interaction [19, 27]. TLR5 signaling on epithelial cells, as well as the direct signaling through TLR5 on DC, could play a role in dendrite formation [31].

The adjuvant activity of flagellin has been shown to be mediated by activation of CD11c+ DC via TLR5 signaling that also leads to enhanced antigen uptake [32]. In the current studies, flagellin-modified CS constructs were readily taken up by murine DC *in vitro*, with the internalized CS antigen distributed either in small and large vesicles, presumably early/late endosomes, or throughout the cytosol (Figures 9, S2). Cytosolic distribution has been observed with other flagellin-modified antigens [4, 33]. The adjuvant activity of alum is dependent on destabilization of lysosome membranes and leakage into the cytosol with subsequent activation of the NRLP3 inflammasome [34]. Cytosolic flagellin injected by TIII secretion system of intracellular *Salmonella* is known to activate the NLRC4 (IPAF) inflammasome leading to host cell death by pyroptosis [35, 36]. The pycnotic nuclei noted in cells with large amounts of cytosolic CS antigen (Figure S2) is consistent with inflammasome-induced pyroptosis and the role of the inflammasome in the adjuvant activity of flagellin remains to be explored.

Presence of the flagellin-modified CS in the cytosol may mimic the cytosolic localization of native CS protein, which is shed by the sporozoite into the cytoplasm during traversal of Kupffer cells and invasion of liver hepatocytes [37, 38]. Murine CS -specific CD8+ cells elicited by immunization with irradiated sporozoites, as well as a *Salmonella*-vectored CS protein vaccine, were protective in murine malaria models [39, 40]. However, CS specific CD8+ T cells were not detected in flagellin-modified CS immunized mice (Carapau, Mitchell, Nacer, Shaw, Othoro, Frevert et al, unpublished), consistent with the inability of C57BL/6 (H-2^b) mice to mount class I restricted responses to CS proteins [41, 42]. Nevertheless, the cytosolic distribution of antigen detected in these studies is consistent with the ability of flagellin modified bacterial and viral antigens to elicit protective CD8+ T cell mediated immunity [4, 33].

Protection in the flagellin-modified CS immunized mice was found to correlate with sporozoite neutralizing antibodies that reduced parasite burden *in vitro* and *in vivo* following challenge with rodent parasites expressing *P. falciparum* CS repeats (Carapau, Mitchell, Nacer, Shaw, Othoro, Frevert et al, unpublished). The imaging of the NALT in the flagellin-modified CS immunized mice emphasizes the challenges of intranasal vaccination and suggest several strategies to enhance IN induced malaria specific humoral immunity. The mucociliary environment within the NALT, provided by the ciliated epithelial cells and mucous producing goblet cells (Figure 8), functions in rapid clearance of inhaled material, which, unfortunately, includes intranasally delivered vaccines. That limited antigen uptake was a factor in immunogenicity of the flagellin-modified CS is suggested by the need for four to five IN doses to elicit peak antibody responses (Carapau, Mitchell, Nacer, Shaw, Othoro, Frevert et al, unpublished). The use of mucoadhesive adjuvants such as chitosan, a cationic copolymer of N-acetylglucosamine and glucosamine derived from crustacean shells that readily binds to the negatively charged nasal mucin, has been successfully used to

enhance immunogenicity of intranasal vaccines [43-45]. The chitosan particulate formulations served both to prolong antigen residence time within the nasal cavity and to enhance uptake by APC. Our recent studies have shown that SC or IM immunization with *P. falciparum* CS microparticles can elicit enhanced anti-repeat antibody and T cell responses in mice and non-human primates [46, 47]. These recent findings suggest that particulate formulations of flagellin-CS combined with a mucoadhesive adjuvant such as chitosan, would improve delivery and uptake of CS vaccines in the NALT. In addition, although the specific roles of M cells and CD11c+ DC, as well as DC sampling of luminal antigen, in immunogenicity of IN delivered flagellin-CS proteins remain to be defined, targeting of NALT APC may further enhance immunogenicity. NALT M cells were specifically labeled with the GS-IB4 lectin (Figure 8) and the addition of lectin tags to target antigens to M cells has been shown to enhance immunogenicity of intranasal viral vaccines [48]. In addition, the inclusion of a DC specific nasal adjuvant, such as the fms-like tyrosine kinase 3 ligand (Flt3L), has been shown to increase NALT DC numbers and expression of co-stimulatory molecules and systemic antibody responses to IN recombinant protein vaccines [49] and may further enhance immunogenicity of IN flagellin-modified CS vaccines.

An optimized IN needle-free malaria vaccine would enable mass immunization campaigns for control of epidemic and endemic malaria and facilitate malaria eradication efforts by reducing costs and eliminating the need for medical personnel to administer the vaccine. In humans, the functional correlate of the rodent NALT is the Waldeyer's ring, a morphologically distinct lymphoid structure composed of the nasopharyngeal adenoid and pairs of palatine, tubal, and lingual tonsils [29]. The Waldeyer's ring is well developed during childhood, and thus nasal vaccines may be particularly promising for infants and young children who are at highest risk of severe *P. falciparum* malaria and death. Recent Phase III trial clinical trials of RTS,S, which is administered IM in a potent liposome adjuvant formulation, have shown protection against clinical disease in 30-55% of immunized infants [1, 2] and efforts to improve immunogenicity are ongoing. Optimization of CS-based immunogens and new delivery methods, such IN immunization, will advance efforts to provide easily administered, potent malaria vaccines for the 40% of the world's population currently at risk of malaria infection.

Methods

Ethics statement

This study was conducted in accordance with the Guide for the Care and Use of Laboratory Animals of the National Institutes of Health. The protocol was approved by the Institutional Animal Care and Use Committee of NYU School of Medicine. All surgery was performed under ketaminexylazine-acepromazine anesthesia and all efforts were made to minimize suffering.

Flagellin-modified *P. falciparum* CS proteins

Design, production and purification of flagellin-modified *P. falciparum* constructs were performed as described for flagellin-modified bacterial and viral vaccines [3-5]. Two *E. coli* expressed fusion proteins were constructed, STF2Δ.CS and STF2.(T1BT*), based on the *P.*

falciparum CS protein (Figure 1). STF2Δ.CS was comprised of nearly full-length *P. falciparum* CS fused to the C-terminus of a truncated *Salmonella enterica* serovar Typhimurium type B flagellin (*Flij*) that lacks 300 aa of the hypervariable hinge region (STF2Δ). The second construct, STF2.(T1BT*), contained full-length *S. enterica* Typhimurium flagellin (STF2) fused to a tri-epitope sequence representing immunodominant T and B cell epitopes of *P. falciparum* CS protein recognized by sera and cells of immunized individuals. The purified flagellin-modified CS constructs contained <0.01 EU/μg endotoxin levels, based on a Limulus Amoebocyte Lysate (LAL) kit QCL 1000 (Cambrex, Walkersville, MD), and stimulated cytokine production by cells transfected with a human TLR5 gene.

Immunization

C57BL/6 and BALB/c mice (Jackson Laboratories, Bar Harbor, ME) were housed in AALAC approved Animal Facilities according to NYU School of Medicine IACUC approved protocols. Mice ≥8 weeks were used as nasopharynx-associated lymphoid tissue organogenesis does not begin until after birth and reaches maturation at ∼8 weeks of age [14]. Mice were immunized at two-week intervals with 10 – 50 μg of flagellin-modified CS by placing 10 μl in each nare of anesthetized mice. Controls included mice immunized IN with full-length or truncated flagellin without CS (STF2, STF2Δ) or with PBS.

DC cultivation

Murine bone marrow-derived DC (BMDC), obtained from the tibias and femurs of naïve mice, were filtered through a 100 μm mesh (Corning Life Sciences, Oneonta, NY) and the red cells were lysed. The washed cell pellet was resuspended in complete DMEM supplemented with 30% conditioned medium obtained from cultures of Ag8653 cells transfected with recombinant GM-CSF (provided by Dr. Ana Rodriguez, New York University). Cells were cultured at 37°C, 5% CO_2 and humid atmosphere, and medium was changed every other day.

To assess antigen uptake, murine BMDC were plated into 8-well Permanox Lab-Tek chamber slides plates at 2×10^5 per well and incubated with 10 or 100 μg/ml STF2Δ.CS or STF2.(T1BT*)$_{4\times}$ at 4°C for 30 min to allow synchronized binding, followed by incubation at 37°C to allow antigen uptake. Cells were fixed *in situ* with 4% paraformaldehyde in PBS and permeabilized with 0.25% Triton X-100 in PBS. Intracellular antigen was detected by labeling with 10 μg/ml mAb 2A10, specific for *P. falciparum* CS protein, followed by biotinylated goat anti-mouse IgG (Invitrogen, Eugene, OR), and streptavidin-Qdots 655 (Invitrogen). Nuclei were stained with Hoechst 33342 (Invitrogen).

NALT preparation

NALTs were removed from immunized or naïve mice using a standard protocol [50]. To visualize the position of the NALTs on the cranial side of the upper palate, mice were anesthetized by intraperitoneal injection of a cocktail of 50 mg/kg ketamine (Ketaset, Fort Dodge Animal Health, Fort Dodge, IO), 10 mg/kg xylazine (Rompun, Bayer, Shawnee Mission, KS), and 1.7 mg/kg acepromazine (Boehringer Ingelheim Vetmedica, St. Joseph, MO) (KXA mix) [51]. Mice were intravenously injected with 100 μl of a 1% Evans blue

solution in PBS and sacrificed 3 h later. NALTs were either dissected from the palate or analyzed *in situ*. Specimens were photographed with a Leica MZ16 FA stereomicroscope equipped with a Leica DFC 300 FX camera. Data were imported into Adobe Photoshop Elements for further processing.

NALT histology

NALTs from naïve mice were fixed with 1% glutaraldehyde in PBS, postfixed with 1% OsO_4 and 1.5% $K_3Fe(CN)_6$, stained *en bloc* with 0.5% uranyl acetate, dehydrated in ethanol, and embedded in Epon. Semithin sections were stained with toluidine blue. For morphological comparison of NALTs from immunized and naïve mice, noses were separated from the head, cleaned from connective tissue, fixed for 24 hours in 4% paraformaldehyde in PBS. The snouts were decalcified for 5-6 days in 0.42 M EDTA, pH 7.1 [52] and embedded in paraffin. Sections were stained with trichrome or hematoxylin & eosin. Cryosections were prepared from the same specimens and stained with Giemsa.

NALT draining lymph nodes

To identify changes in the dLN associated with intranasal immunization, mice were administered Higgins Waterproof India Ink (#4425) [53], either in combination with Sigma Ribi Adjuvant System (S6322) or flagellin (STF2). Briefly, the adjuvants were reconstituted/diluted with sterile PBS and mixed 1:1 with India ink. Mice were administered 30 μl (15 μl/nare) of these mixtures, either intranasally or subcutaneously, and sacrificed 14 post first dose or 7 days post second dose. The LN were excised and examined for the presence of ink and changes in size in comparison to control mice.

Immunolabeling and confocal microscopy

For confocal microscopy, the palate was removed, immediately placed NALT-side down into OCT, frozen in liquid nitrogen, and stored at -80°C until further use. Frozen sections cut with a Leica CM 3050S cryostat were briefly immersed in ice-cold acetone, air dried overnight, and stored at -20°C. Slides were fixed with ice-cold acetone and labeled with rat anti-mouse CD45R B220 (clone RA3-6B2; eBioscience, San Diego, CA) to detect B cells, Armenian hamster anti-CD3 (clone 145-2C11; BD Biosciences) to detect T cells and biotinylated anti-CD11c (clone N418; eBioscience) to detect DCs. Secondary antibodies were donkey anti-rat Alex Fluor 488 or 546 (Invitrogen) or anti-Armenian hamster DyLight 488 or 594 (BioLegend, San Diego, CA). Streptavidin Alexa Fluor 633 (Invitrogen) was used to detect biotinylated primary antibodies.

M cells were detected by labeling frozen sections or whole fixed NALTs with the M cell-specific *Griffonia simplicifolia* lectin GS-IB_4 conjugated to Alexa Fluor 568 (Invitrogen). For whole NALT preparations, mice were perfused with heparinized PBS followed by 4% paraformaldehyde in PBS. The palate containing the NALT was removed and fixation continued for 1 h at RT [17]. After washing with PBS, palates were incubated for 1 h with 20 μg/ml GS-IB_4 conjugated to Alexa Fluor 568. NALTs were washed with PBS and imaged immediately by confocal microscopy. Sections were labeled accordingly for 1 h at RT following the manufacturer's instructions (MBL). Blood vessels were labeled with 5 μg/ml mouse anti-CD31 conjugated to Alexa Fluor 647 (BioLegend). Lymph vessels were

detected with 5 μg/ml rat anti-mouse LYVE-1 followed by donkey anti-rat IgG conjugated to Alexa Fluor 488 (Invitrogen).

Specimens were analyzed with an inverted Leica TCS SP2 AOBS confocal system and 2D and 3D data acquired with Leica Confocal Software. Imaris 7.4 (Bitplane, Saint Paul, MN), Image-Pro Plus (Media Cybernetics, Bethesda, MD), AutoDeBlur (Media Cybernetics, Bethesda, MD), and NIH ImageJ were used for further image processing and deconvolution.

Flow cytometry

After removal from the palate, NALTs from three mice within each group were pooled and transferred into RPMI supplemented with 15% fetal bovine serum (FBS) (HyClone, Logan, UT). Individual cells were obtained by filtering NALTs through a 100 μm sieve (Corning, Corning, NY). Cells were incubated 30 min on ice with a 1:200 dilution of Fc block (CD16/32, BD Biosciences) in FACS buffer (3% FBS in PBS). Lymphocyte populations were detected for 30 min on ice with APC-conjugated anti-mouse CD3ε antibody (clone 145-2C11, BioLegend), APC-conjugated anti-mouse CD11c (clone N418, BioLegend), and PerCP/Cy5.5-conjugated rat anti-mouse B220 (clone RA3-6B2, BioLegend), diluted 1:100 in FACS buffer followed by fixation with 4% paraformaldehyde in PBS. Data were acquired with a FACSCaliber cytometer (Beckton-Dickson, Franklin Lakes, NJ) and analyzed with FlowJo software (Tree Star, Inc., Ashland, OR).

Statistics

One-way ANOVA and one-tailed t-test analyses were performed with GraphPad Prism® 5.04.

Supplementary Material

Refer to Web version on PubMed Central for supplementary material.

Acknowledgments

VaxInnate is acknowledged as a source of the flagellin-modified CS proteins and we thank A. Price and V. Nakaar for production and purification of the flagellin and flagellin-modified CS proteins. The work was supported by NIH/NIAID grant R56 AI083655 to EN and NIH/NCRR grant S10 RR019288 to UF. We thank John Bates, Wake Forest University School of Medicine, for valuable discussions. Trichrome and H&E staining of paraffin embedded specimens was done at the Histopathology Core Facility of New York University School of Medicine.

References

1. Agnandji ST, et al. First results of phase 3 trial of RTS,S/AS01 malaria vaccine in African children. N Engl J Med. 2011; 365(20):1863–75. [PubMed: 22007715]
2. Agnandji ST, et al. A phase 3 trial of RTS,S/AS01 malaria vaccine in African infants. N Engl J Med. 2012; 367(24):2284–95. [PubMed: 23136909]
3. Huleatt JW, et al. Potent immunogenicity and efficacy of a universal influenza vaccine candidate comprising a recombinant fusion protein linking influenza M2e to the TLR5 ligand flagellin. Vaccine. 2008; 26(2):201–14. [PubMed: 18063235]
4. Huleatt JW, et al. Vaccination with recombinant fusion proteins incorporating Toll-like receptor ligands induces rapid cellular and humoral immunity. Vaccine. 2007; 25(4):763–75. [PubMed: 16968658]

5. McDonald WF, et al. A West Nile virus recombinant protein vaccine that coactivates innate and adaptive immunity. J Infect Dis. 2007; 195(11):1607–17. [PubMed: 17471430]
6. Taylor DN, et al. Development of VAX128, a recombinant hemagglutinin (HA) influenza-flagellin fusion vaccine with improved safety and immune response. Vaccine. 2012; 30(39):5761–9. [PubMed: 22796139]
7. Taylor DN, et al. Induction of a potent immune response in the elderly using the TLR-5 agonist, flagellin, with a recombinant hemagglutinin influenza-flagellin fusion vaccine (VAX125, STF2.HA1 SI). Vaccine. 2011; 29(31):4897–902. [PubMed: 21596084]
8. Treanor JJ, et al. Safety and immunogenicity of a recombinant hemagglutinin influenza-flagellin fusion vaccine (VAX125) in healthy young adults. Vaccine. 2010; 28(52):8268–74. [PubMed: 20969925]
9. Persson C, et al. Cutting edge: a new tool to evaluate human pre-erythrocytic malaria vaccines: rodent parasites bearing a hybrid Plasmodium falciparum circumsporozoite protein. J Immunol. 2002; 169(12):6681–5. [PubMed: 12471098]
10. Arakawa T, et al. Nasal immunization with a malaria transmission-blocking vaccine candidate, Pfs25, induces complete protective immunity in mice against field isolates of Plasmodium falciparum. Infect Immun. 2005; 73(11):7375–80. [PubMed: 16239536]
11. Bargieri DY, et al. New malaria vaccine candidates based on the Plasmodium vivax Merozoite Surface Protein-1 and the TLR-5 agonist Salmonella Typhimurium FliC flagellin. Vaccine. 2008; 26(48):6132–42. [PubMed: 18804504]
12. Romero JF, et al. Intranasal administration of the synthetic polypeptide from the C-terminus of the circumsporozoite protein of Plasmodium berghei with the modified heat-labile toxin of Escherichia coli (LTK63) induces a complete protection against malaria challenge. Vaccine. 2009; 27(8):1266–71. [PubMed: 19111883]
13. Hirunpetcharat C, et al. Intranasal immunization with yeast-expressed 19 kD carboxyl-terminal fragment of Plasmodium yoelii merozoite surface protein-1 (yMSP119) induces protective immunity to blood stage malaria infection in mice. Parasite Immunol. 1998; 20(9):413–20. [PubMed: 9767608]
14. Harmsen A, et al. Cutting edge: organogenesis of nasal-associated lymphoid tissue (NALT) occurs independently of lymphotoxin-alpha (LT alpha) and retinoic acid receptor-related orphan receptor-gamma, but the organization of NALT is LT alpha dependent. J Immunol. 2002; 168(3):986–90. [PubMed: 11801629]
15. Elmore SA. Enhanced histopathology of mucosa-associated lymphoid tissue. Toxicol Pathol. 2006; 34(5):687–96. [PubMed: 17067953]
16. Tripp CH, et al. The lymph vessel network in mouse skin visualised with antibodies against the hyaluronan receptor LYVE-1. Immunobiology. 2008; 213(9-10):715–28. [PubMed: 18926287]
17. Takata S, Ohtani O, Watanabe Y. Lectin binding patterns in rat nasal-associated lymphoid tissue (NALT) and the influence of various types of lectin on particle uptake in NALT. Arch Histol Cytol. 2000; 63(4):305–12. [PubMed: 11073062]
18. Rescigno M, et al. Dendritic cells express tight junction proteins and penetrate gut epithelial monolayers to sample bacteria. Nat Immunol. 2001; 2(4):361–7. [PubMed: 11276208]
19. Niess JH, et al. CX3CR1-mediated dendritic cell access to the intestinal lumen and bacterial clearance. Science. 2005; 307(5707):254–8. [PubMed: 15653504]
20. Calvo-Calle JM, et al. A linear peptide containing minimal T- and B-cell epitopes of Plasmodium falciparum circumsporozoite protein elicits protection against transgenic sporozoite challenge. Infect Immun. 2006; 74(12):6929–39. [PubMed: 17030584]
21. Kastenmuller K, et al. Full-Length Plasmodium falciparum Circumsporozoite Protein Administered with Long-Chain Poly(I{middle dot}C) or the Toll-Like Receptor 4 Agonist Glucopyranosyl Lipid Adjuvant-Stable Emulsion Elicits Potent Antibody and CD4+ T Cell Immunity and Protection in Mice. Infect Immun. 2013; 81(3):789–800. [PubMed: 23275094]
22. Cashman SB, Morgan JG. Transcriptional analysis of Toll-like receptors expression in M cells. Mol Immunol. 2009; 47(2-3):365–72. [PubMed: 19781788]
23. Costalonga M, et al. Intranasal bacteria induce Th1 but not Treg or Th2. Mucosal Immunol. 2009; 2(1):85–95. [PubMed: 19079337]

24. Park HS, et al. Primary induction of CD4 T cell responses in nasal associated lymphoid tissue during group A streptococcal infection. Eur J Immunol. 2004; 34(10):2843–53. [PubMed: 15368301]
25. Kraehenbuhl JP, Neutra MR. Epithelial M cells: differentiation and function. Annu Rev Cell Dev Biol. 2000; 16:301–32. [PubMed: 11031239]
26. Sierro F, et al. Flagellin stimulation of intestinal epithelial cells triggers CCL20-mediated migration of dendritic cells. Proc Natl Acad Sci U S A. 2001; 98(24):13722–7. [PubMed: 11717433]
27. Chieppa M, et al. Dynamic imaging of dendritic cell extension into the small bowel lumen in response to epithelial cell TLR engagement. J Exp Med. 2006; 203(13):2841–52. [PubMed: 17145958]
28. Rescigno M. Functional specialization of antigen presenting cells in the gastrointestinal tract. Curr Opin Immunol. 2010; 22(1):131–6. [PubMed: 20060698]
29. Ogasawara N, et al. Epithelial barrier and antigen uptake in lymphoepithelium of human adenoids. Acta Otolaryngol. 2011; 131(2):116–23. [PubMed: 21062118]
30. Takano K, et al. HLA-DR- and CD11c-positive dendritic cells penetrate beyond well-developed epithelial tight junctions in human nasal mucosa of allergic rhinitis. J Histochem Cytochem. 2005; 53(5):611–9. [PubMed: 15872054]
31. Uematsu S, et al. Regulation of humoral and cellular gut immunity by lamina propria dendritic cells expressing Toll-like receptor 5. Nat Immunol. 2008; 9(7):769–76. [PubMed: 18516037]
32. Bates JT, et al. Direct stimulation of tlr5+/+ CD11c+ cells is necessary for the adjuvant activity of flagellin. J Immunol. 2009; 182(12):7539–47. [PubMed: 19494277]
33. Cuadros C, et al. Flagellin fusion proteins as adjuvants or vaccines induce specific immune responses. Infect Immun. 2004; 72(5):2810–6. [PubMed: 15102791]
34. Li H, et al. Cutting edge: inflammasome activation by alum and alum's adjuvant effect are mediated by NLRP3. J Immunol. 2008; 181(1):17–21. [PubMed: 18566365]
35. Franchi L, et al. Cytosolic flagellin requires Ipaf for activation of caspase-1 and interleukin 1beta in salmonella-infected macrophages. Nat Immunol. 2006; 7(6):576–82. [PubMed: 16648852]
36. Miao EA, et al. Caspase-1-induced pyroptosis is an innate immune effector mechanism against intracellular bacteria. Nat Immunol. 2010; 11(12):1136–42. [PubMed: 21057511]
37. Hugel FU, Pradel G, Frevert U. Release of malaria circumsporozoite protein into the host cell cytoplasm and interaction with ribosomes. Mol Biochem Parasitol. 1996; 81(2):151–70. [PubMed: 8898331]
38. Pradel G, Frevert U. Malaria sporozoites actively enter and pass through rat Kupffer cells prior to hepatocyte invasion. Hepatology. 2001; 33:1154–1165. [PubMed: 11343244]
39. Romero P, et al. Cloned cytotoxic T cells recognize an epitope in the circumsporozoite protein and protect against malaria. Nature. 1989; 341(6240):323–6. [PubMed: 2477703]
40. Sadoff JC, et al. Oral Salmonella typhimurium vaccine expressing circumsporozoite protein protects against malaria. Science. 1988; 240(4850):336–8. [PubMed: 3281260]
41. Hafalla JC, et al. Identification of Targets of CD8(+) T Cell Responses to Malaria Liver Stages by Genome-wide Epitope Profiling. PLoS Pathog. 2013; 9(5):e1003303. [PubMed: 23675294]
42. Doolan DL, Hoffman SL. The complexity of protective immunity against liver-stage malaria. J Immunol. 2000; 165(3):1453–62. [PubMed: 10903750]
43. Sui Z, et al. Cross-protection against influenza virus infection by intranasal administration of M1-based vaccine with chitosan as an adjuvant. Vaccine. 2010; 28(48):7690–8. [PubMed: 20870054]
44. Kobayashi T, et al. Evaluation of the effectiveness and safety of chitosan derivatives as adjuvants for intranasal vaccines. Viral Immunol. 2013; 26(2):133–42. [PubMed: 23509985]
45. Jabbal-Gill I, Watts P, Smith A. Chitosan-based delivery systems for mucosal vaccines. Expert Opin Drug Deliv. 2012; 9(9):1051–67. [PubMed: 22708875]
46. Przysiecki C, et al. Sporozoite neutralizing antibodies elicited in mice and rhesus macaques immunized with a Plasmodium falciparum repeat peptide conjugated to meningococcal outer membrane protein complex. Front Cell Infect Microbiol. 2012; 2:146. [PubMed: 23226683]

47. Powell TJ, et al. Plasmodium falciparum synthetic LbL microparticle vaccine elicits protective neutralizing antibody and parasite-specific cellular immune responses. Vaccine. 2013; 31(15): 1898–904. [PubMed: 23481177]

48. Manocha M, et al. Enhanced mucosal and systemic immune response with intranasal immunization of mice with HIV peptides entrapped in PLG microparticles in combination with Ulex Europaeus-I lectin as M cell target. Vaccine. 2005; 23(48-49):5599–617. [PubMed: 16099080]

49. Kataoka K, et al. The nasal dendritic cell-targeting Flt3 ligand as a safe adjuvant elicits effective protection against fatal pneumococcal pneumonia. Infect Immun. 2011; 79(7):2819–28. [PubMed: 21536790]

50. Heritage PL, et al. Comparison of murine nasal-associated lymphoid tissue and Peyer's patches. Am J Respir Crit Care Med. 1997; 156(4 Pt 1):1256–62. [PubMed: 9351630]

51. Frevert U, et al. Intravital observation of Plasmodium berghei sporozoite infection of the liver. PLoS Biol. 2005; 3(6):e192. [PubMed: 15901208]

52. Sanderson C, Radley K, Mayton L. Ethylenediaminetetraacetic acid in ammonium hydroxide for reducing decalcification time. Biotechnic & histochemistry. 1995; 70(1):12–18. [PubMed: 7540046]

53. Van den Broeck W, Derore A, Simoens P. Anatomy and nomenclature of murine lymph nodes: Descriptive study and nomenclatory standardization in BALB/cAnNCrl mice. J Immunol Methods. 2006; 312(1-2):12–9. [PubMed: 16624319]

Abbreviations

BMDC	bone marrow derived dendritic cells
CS	circumsporozoite protein
dLN	draining lymph node
FAE	follicular associated epithelia
PP	Peyer's Patches
GALT	gastrointestinal associated lymphoid tissue
NALT	nasopharynx-associated lymphoid tissue
STF2	*Salmonella enterica* serovar Typhimurium flagellin B
TLR5	Toll-like receptor 5

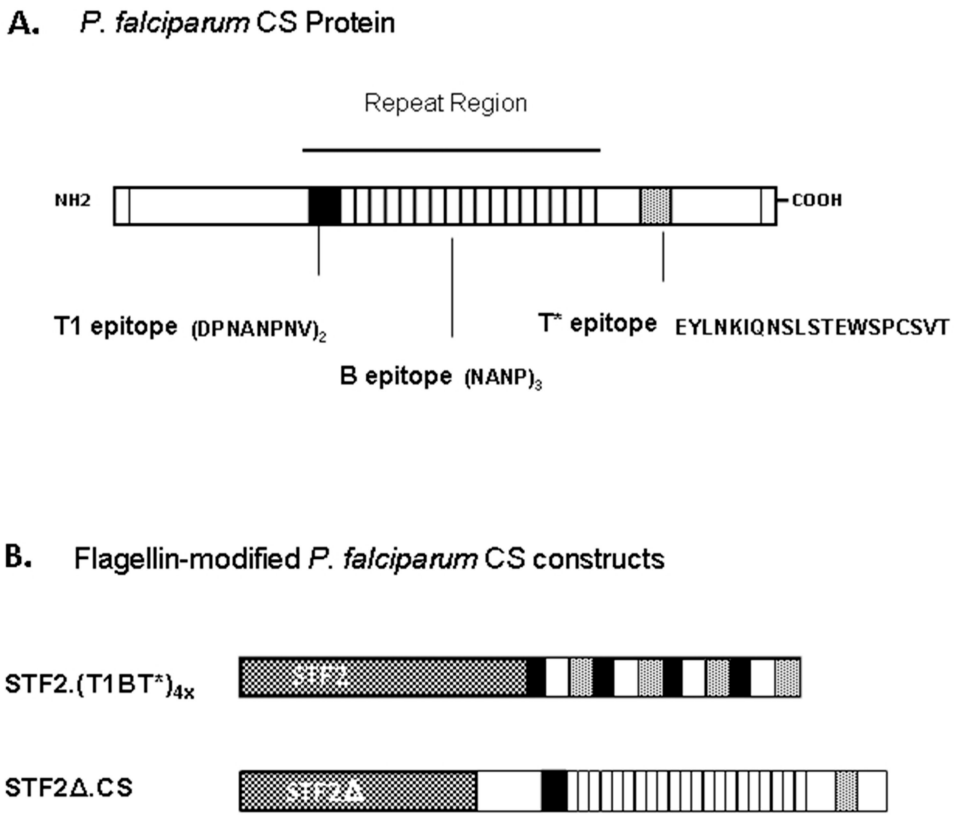

Figure 1.

Diagram of *P. falciparum* CS protein showing (A) location and amino acid sequence of the T1 and B cell epitopes within the central repeat region and the universal CD4+ T helper epitope, T*, in the C-terminus; (B) recombinant STF2 $(T1BT^*)_{4\times}$ comprised of full length flagellin and four copies of the T and B cell epitopes the *P. falciparum* CS protein and STF2Δ. CS comprised of truncated flagellin, lacking the hinge region, and a nearly full length *P. falciparum* CS protein lacking only the N-terminus signal sequence and the C-terminal putative GPI anchor.

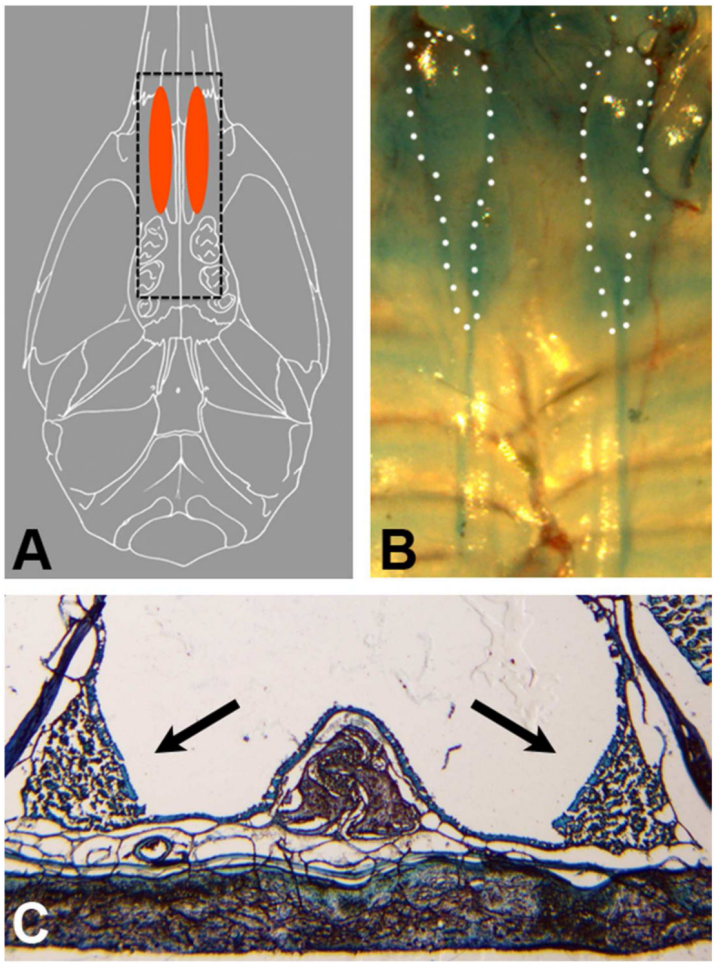

Figure 2. Localization of the NALT on the soft palate

(A) Schematic showing the paired NALT in relation to the palate and the molars. (B) Soft palate from a naïve CBA/Ca mouse that was injected Evans blue to visualize the paired NALT (dotted lines). (C) Cross section of the nasal cavity of a naïve C57BL/6 mouse showing the triangular shape of the NALTs (arrows). NALTs are located on either side of the nasal airways, which are fully separated by the nasal septum in the posterior part of the nose. Giemsa stained frozen section prepared after decalcification of the osseous tissue. Scale bar = 100 μm.

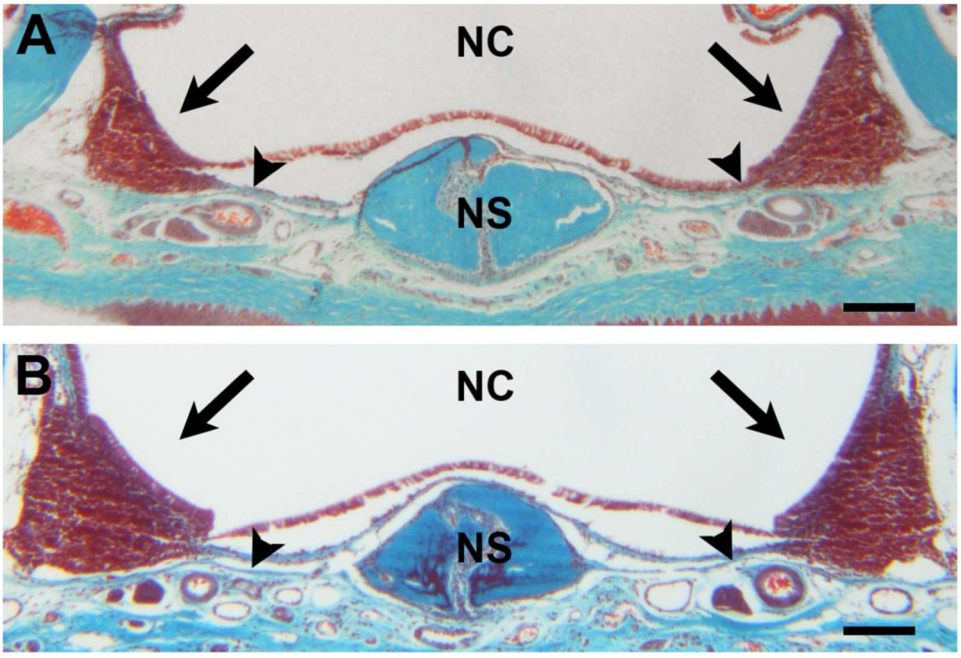

Figure 3. NALT in mice immunized IN with flagellin modified CS

Trichrome-stained cross-sections of the upper palate and nasal cavity showing the paired NALT (arrows) in (A) a naïve C57BL/6 mouse and (B) eight days after the fourth IN immunization with STF2Δ.CS. Paraffin sections were taken between the midpoint of the triangular palate tip and the first molar and reflect a true increase in size rather than an artifact due to section position. Arrowheads = soft palate, NS = nasal septum, NC = nasal cavity. Scale bars = 100 μm.

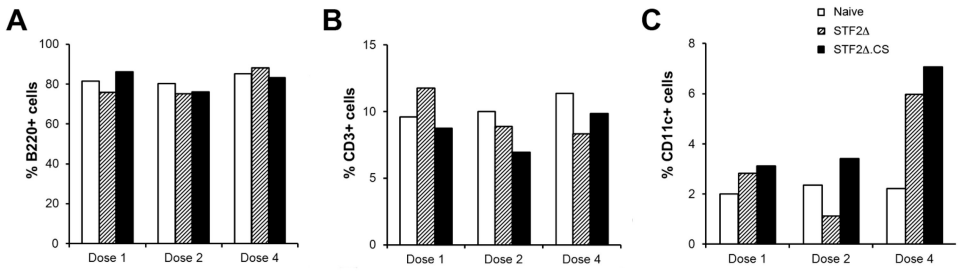

Figure 4. Cellular composition of the NALT following IN immunization with flagellin modified CS protein

Flow cytometric measurement of B, T, and CD11c+ DC present in the NALT of naive C57BL/6 mice or two weeks after IN immunizations with either STF2Δ.CS or flagellin only (STF2Δ). In naïve mice (time point Dose 1), the percentage of B cells (A), T cells (B), and DC (C) account for roughly 80%, 10%, and 2% of the total cell population of the NALT, respectively. While the T:B ratio did not change in the immunized mice, the number of DC increased after immunization with both flagellin-modified CS and with flagellin only. Shown are representative results from one experiment in which NALT were excised from three naïve or IN immunized mice and cells pooled for flow cytometric analysis.

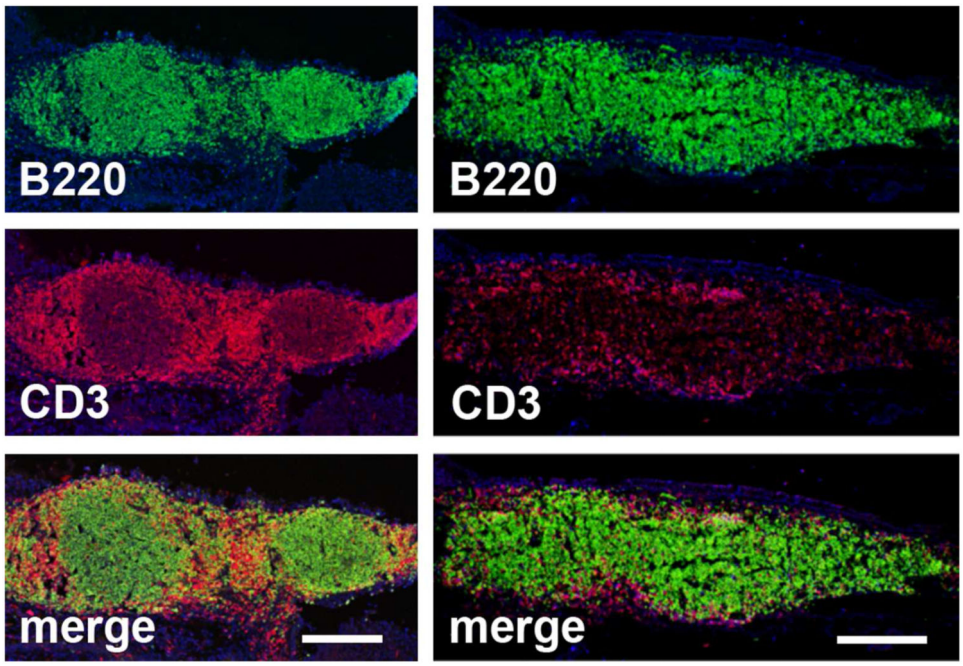

Figure 5. Lymphocyte distribution in the NALT

Representative NALT from a naïve C57BL/6 mouse (left panels) and a C57BL/6 mouse two weeks after IN immunization with four doses of STF2.$(T1BT^*)_{4\times}$ (right panels). Longitudinal sectioning reveals the organization of B cells (B220, green) in germinal centers, while T cells (CD3, red) occupy mainly the periphery of the B cell GC areas. B cells were labeled with rat anti-mouse B220 followed by anti-rat Alexa Fluor 488, T cells with hamster anti-mouse CD3 followed by anti-hamster IgG DyLight 594. Nuclei were stained with Hoechst (blue). The anterior portion of the NALTs is on the right, the epithelium on top. Scale bars = 200 μm.

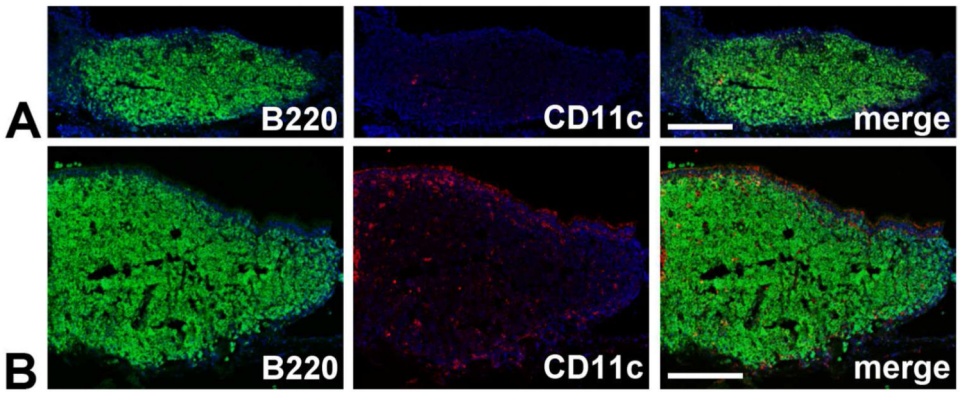

Figure 6. NALT DC in mice immunized IN with flagellin modified CS

NALT from (A) naïve C57BL/6 mouse and (B) two weeks after IN immunization with four doses of STF2.$(T1BT^*)_{4\times}$. While CD11c+ DC (red) are rare in (A) naïve NALT, (B) after IN immunization, the size of the NALT and number of DC is increased significantly. DC were detected with biotinylated anti-mouse CD11c followed by streptavidin Alexa Fluor 633 (red), and B cells with rat anti-mouse B220 followed by anti-rat Alexa Fluor 488 (green). Nuclei were stained with Hoechst (blue). The anterior portion of the NALTs is on the right, the epithelium on top. Scale bars = 200 μm.

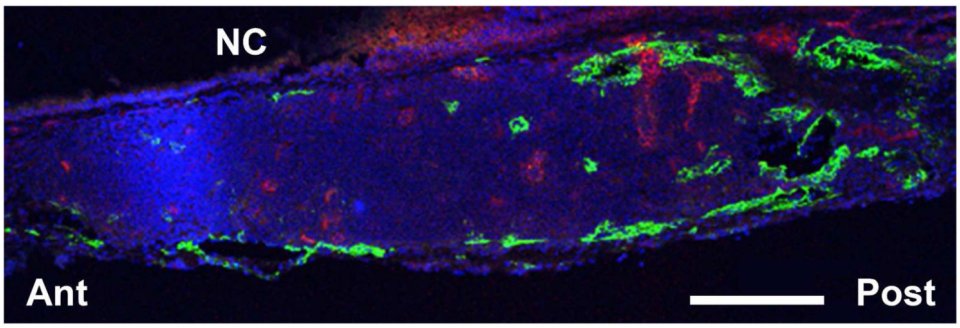

Figure 7. Blood supply and lymphatic drainage of the NALT

Longitudinal section through a NALT from a C57BL/6 mouse 10 min after IN administration of STF2.$(T1BT^*)_{4\times}$. Lymphatic endothelia were stained with rat anti-mouse LYVE-1 followed by anti-rat IgG conjugated to Alexa Fluor 488 (green), blood vessel endothelia were detected with rat anti-mouse PECAM-1 conjugated to Alexa Fluor 647 (red). Nuclei were stained with Hoechst (blue). NC = nasal cavity, Ant = anterior, Post = posterior. Scale bar = 100 μm.

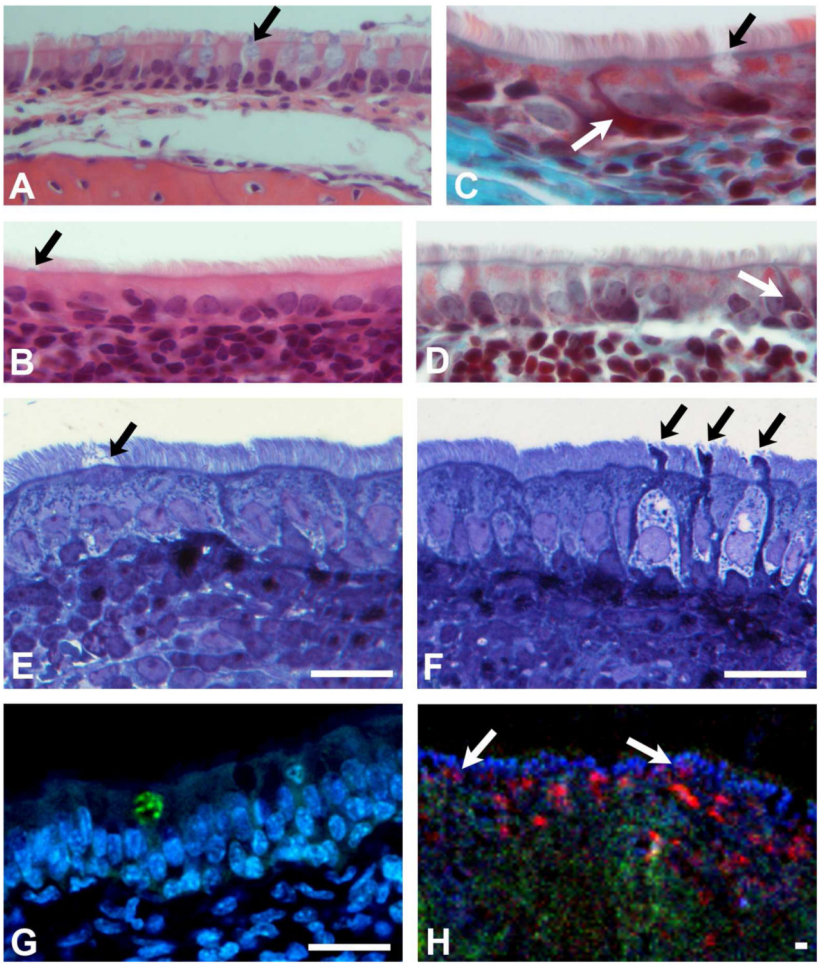

Figure 8. Composition of the epithelium covering the NALT

H&E-stained paraffin sections demonstrate that while the epithelium that lines the majority of the nasal cavity contains a large number of goblet cells (A, black arrow), these mucus-secreting cells are rare in the epithelium covering the NALT (B, black arrow). M cells, which are typically located in the apical portion of the NALT epithelium, can be identified by the lack of cilia (C, black arrow). In trichrome-stained paraffin sections (C, D) and toluidine blue-stained Epon sections (E, F), occasionally, cells of a dendritic shape can be found, whose dendrites extend across the epithelium into the nasal cavity (C and D, white arrows; F, black arrows), in addition to M cells (E, black arrow). (G) By confocal microscopy, M cells (green) were located apical from the epithelial nuclei (blue). M cells were labeled with GS-IB_4 lectin conjugated to Alexa Fluor 568, nuclei were stained with Hoechst. (H) The majority of the CD11c+ DC (red) were located in the sub-epithelial portion of the lymphoid tissue, while some DC have infiltrated the epithelium (white arrows). DC were detected by confocal microscopy using biotinylated anti-mouse CD11c followed by streptavidin Alexa Fluor 633. Scale bars = 10 μm.

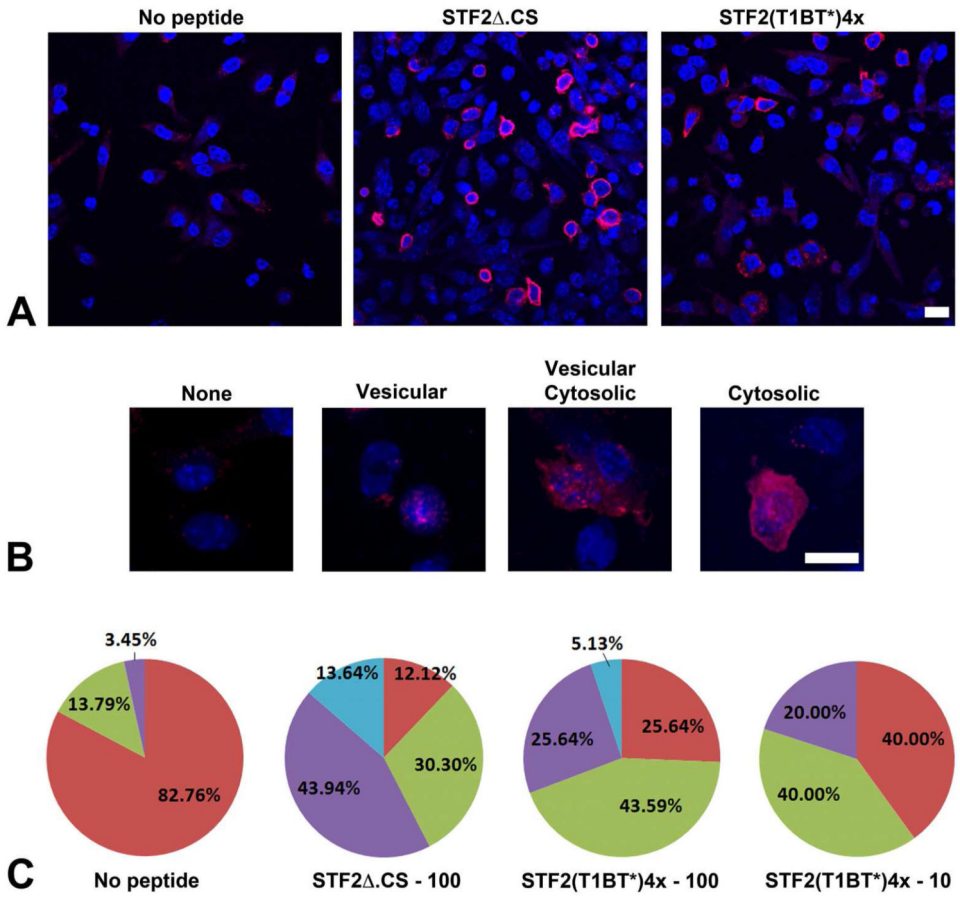

Figure 9. Uptake of flagellin-modified CS constructs by DC

(A) Murine BMDC were incubated for 30 min on ice with no peptide, 100 μg/ml STF2Δ.CS or 100 μg/ml of STF2.(T1BT*)$_{4\times}$. Subsequently, cells were allowed to internalize the proteins for 30 min at 37°C. After fixation and permeabilization, intracellular CS was detected by staining with mAb 2A10, specific for *P. falciparum* CS protein repeats, followed by biotinylated goat anti-mouse IgG and streptavidin-Qdots 655 (red). Nuclei were stained with Hoechst (blue). (B) After 30 min incubation with 100 μg/ml STF2Δ.CS, the intracellular peptide labeling pattern in BMDC ranges from vesicular and vesicular/cytosolic labeling, to uniform distribution throughout the cytosol. Scale bars = 10 μm. (C) Percentage of cells labeled with MAB 2A10 after 30 min of incubation without peptide, with 100 μg/ml STF2Δ.CS or with 100 μg/ml or 10 μg/ml of STF2.(T1BT*)$_{4\times}$. No staining (red), vesicular (green), vesicular/cytosolic (purple), or predominantly cytosolic labeling pattern (blue). Data represent a total of 300-500 cells counted per experimental condition.